Green Chemistry

PAPER

View Article Online
View Journal | View Issue

Cite this: *Green Chem.*, 2024, **26**, 3378

Green liquid marble-based hydrogels as pesticidal pyrethrin slow-release carriers†

Qin Li,‡[a] Changhong Wang,‡[a] Jiayuan He,[a] Dandan Yang,[a] Ting Li,[a] Huixian Xu,[a] Weifeng Shen,[a] Liandi Zhou,*[b] Saimeng Jin,*[a] Qihui Zhang*[a] and James H. Clark[c]

Pyrethrins are effective agents against mosquito larvae, but their rapid degradation rate in water reduces their deinsectization efficiency and increases the cost of deinsectization. Based on liquid marbles, a biodegradable slow-release hydrogel carrier is prepared using green and low-cost materials for the slow release of natural pyrethrin on water surfaces to kill mosquito larvae. Green carriers with high stability and loading of high concentrations of pyrethrin are synthesized by cross-linking Ca^{2+} in 5% $CaCl_2$ solution with sodium alginate. The superior stability of liquid marbles at the water surface and the electrostatic interaction between alginate and gelatin can effectively reduce the degradation rate of pyrethrin in water. Furthermore, the carrier system displayed a long sustained-release time (>144 h) and maintained larvicidal performance after 168 h. Good floating stability is demonstrated for the liquid marble hydrogels. The larvicidal activity of the obtained drug carrier reached 100% with different water volumes but the same dosage. This work provides a strategy to exterminate mosquito larvae with high efficiency by preparing a green hydrogel drug slow-release carrier, thus providing a new approach to expanding the application of liquid marbles in green chemistry.

Received 25th September 2023,
Accepted 22nd January 2024

DOI: 10.1039/d3gc03625a

rsc.li/greenchem

1. Introduction

Mosquitoes are one of the main culprits in spreading malaria and other diseases, including dengue, chikungunya, yellow fever and Zika virus.[1] In the open water system, the population of mosquito larvae can be controlled by various predators, including tadpoles, water bugs, fish, copepods and crabs.[2] However, the smell from stagnant pools can attract mosquitoes to lay eggs, which hatch to release larvae.[3] Therefore, mosquitoes often thrive in small stagnant waterholes.[4] Organophosphates, microbial agents and insect growth regulators are normally applied to directly target mosquitoes; however, these agents are highly toxic or expensive.[5] Some researchers have developed methods that use nanomaterials to block the mosquito life cycle.[6,7] Parvin *et al.* developed a non-toxic nanoparticle coated with carbon to kill mosquito larvae after a long period of stagnation in the larval stage.[8] As mosquito larvae (also known as worms) hang upside down below the surface of water and breathe at the surface with the end of their tails, the release of insecticides at the surface of water is an effective means of mosquito extermination. However, few studies have described a way to control mosquitoes based on the behaviour of the larvae.

Pyrethrin is a green biocide derived from pyrethrum flowers and has been used against mosquitoes for a long time. Natural pyrethrin is effective in eradicating a wide range of insects and is considered less toxic to mammals and other non-target organisms.[9] Compared to synthetic insecticides, natural pyrethrin is eco-friendly with a very short half-life in natural environment.[10] Because of the degradation and deactivation of pyrethrin in sunlight and air,[11] it does not pose a risk to humans and the environment. Despite its lipophilic properties, natural pyrethrin degrades rapidly in water and leaves no residue in water sediments or fish tissue.[12] Rapid degradation leads to increased release frequency, dosage, and cost of pyrethrin, resulting in difficulty in mosquito control. Thus, a continuous and controlled mode for pyrethrin release needs to be developed to achieve an expected larvicidal efficacy and avoid the evaporation or early degradation of pyrethrin.

Early studies have provided some methods that are used to solve the above problems. Researchers prepared pyrethrin formulations in which pyrethrin was loaded with natural poly-

[a]*School of Chemistry and Chemical Engineering, Chongqing University, Chongqing, 400044, China. E-mail: qhzhang@cqu.edu.cn, sj708@cqu.edu.cn*
[b]*Chongqing College of Traditional Chinese Medicine, Chongqing 402760, China. E-mail: zhouliandi@cqctcm.edu.cn*
[c]*Circa Renewable Chemistry Institute, Green Chemistry Centre of Excellence, University of York, York, YO10 5DD, UK*

†Electronic supplementary information (ESI) available: Supporting experimental procedures, supporting Figures, supporting tables. See DOI: https://doi.org/10.1039/d3gc03625a

‡These authors contributed equally to this work.

mers,[13] inorganic non-metallic materials[14] and nano-mixed micelles.[15–17] Among various natural polymers, alginates are used extensively in the preparation of hydrogel microspheres, micro-capsules and membranes for controlled drug release because of their biocompatible, biodegradable and nontoxic properties.[18–20] In addition, alginates can be formed as ionotropic hydrogels in the presence of Ca^{2+}, Ba^{2+}, Fe^{3+} and other divalent or trivalent cations.[21] Gelatin is a natural addition for preparing a drug carrier because of its unique characteristics, including nontoxic, edible, biodegradability and low cost.[22] Some reports suggested that there exists electrostatic interaction between the groups of gelatin and alginates, which favors the stability of emulsion.[23,24] Therefore, alginates and gelatin were selected as the aqueous phase to prepare the pyrethrin formulation.

Liquid marble is a natural phenomenon generally associated with the activity in that aphids transformed liquids into soft non-stick solids using wax-like substances.[25] In 2001, Aussillous and Quere first named the shell–core type droplet as liquid marbles and reported on it systematically.[26] Theoretically, the grains that encapsulate droplets can be any particle size less than a few hundred microns, such as silica particles, carbon nanotubes, and cellulose.[27] The surface energy of the droplet will be reduced after covering the non-hydrophilic powder. Consequently, the globular liquid marbles maintain their original shapes, and the contact surface is not moistened, which makes liquid marbles stable in the air or water surface.[28] Owing to these properties, such as easy preparation, wide source of raw materials, non-wetting and good elasticity, liquid marbles have gained increasing attention and are widely used in fields of cosmetics, microfluidics, microreactors and biopharmaceuticals.[29–34] However, limited by their poor mechanical stability, up to now, liquid marbles have rarely been used in the agriculture sector to release pesticide.[35]

Herein, the advantages of liquid marbles and the habit of mosquito larvae were exploited, using green substances, such as cellulose, sodium alginate and gelatin, to design a hydrogel drug carrier to kill *Aedes albopictus* larvae continuously and chronically with fewer doses (Scheme 1). The sodium alginate solution and gelatin solution were mixed and then homogenized with pyrethrin to obtain a pyrethrin emulsion. Then, the pyrethrin emulsion was dropped onto the modified cellulose powder by pipette to prepare liquid marble. Subsequently, the liquid marble was placed on a 5% $CaCl_2$ solution, and the liquid marble-based hydrogel was obtained by water exchange. The formation of hydrogels efficiently overcomes the mechanical instability of liquid marble. Simultaneously, the modified cellulose on the liquid marble-based hydrogels makes them float on the water, releasing pyrethrin to kill wigglers.

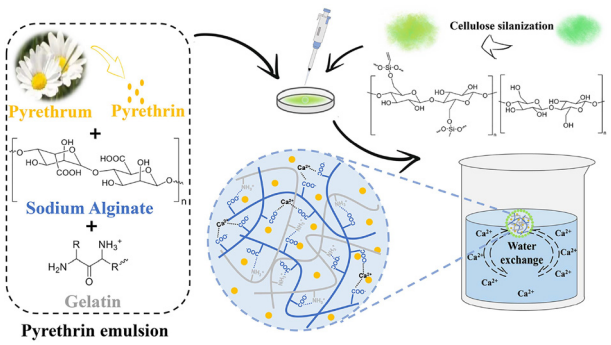

Scheme 1 Preparation process of liquid marble hydrogel loaded pyrethrin.

2. Materials and methods

2.1 Materials

Sodium alginate (SA, 98%) was obtained from Shanghai Yuanye Bio-Technology Co. (Shanghai, China). Gelatin (GE, 99%) was obtained from Damao Chemical Reagent Co. (Tianjin, China). Calcium chloride anhydrous ($CaCl_2$, 96%) and vinyltriethoxysilane (VTES, 97%) were obtained from Aladdin Reagent Co. (Shanghai, China). Ethanol (EtOH, 99%) and sodium hydroxide (NaOH, 98%) were obtained from Kelong Chemicals Co. (Chengdu, China). Cellulose (99%) was obtained from Macklin Biochemical Co. (Shanghai, China). The pyrethrin technology (Py, 50.8%) was obtained from Nanbao Company Co. (Yunnan, China). Pyrethrin (80%) was obtained from Cato Research Chemicals, Inc. (America).

The Aedes albopictus larvae were obtained from the Center for Disease Control and Prevention (Zhejiang, China).

2.2 Synthesis of composites

2.2.1 Silanization of cellulose. 0.3 g of cellulose and 9 mL of 0.1 M NaOH were dispersed in 50 mL of ethanol. Subsequently, 0.3 g of VTES was placed in the cellulose suspension and mixed for 90 min. Then, the modified cellulose was cured at 100 °C for 60 min. After that, the modified cellulose in suspension was obtained by centrifugation (8000 rpm, 5 min). The residue was washed with ethanol three times and centrifuged to remove the supernatant after every washing step. Finally, the modified cellulose was dried under vacuum at 50 °C for 12 h.

The water contact angles (WCAs) were measured by dropping 5 μL deionized water onto the cellulose powder surface, which was pressed on a glass slide. The average value of the three measurements at different spots was the final WCA of each group.

2.2.2 Preparation of liquid marble. A droplet was dropped onto the modified cellulose powder, and the container was shaken slightly. Liquid drops of different sizes were generated using a pipette to form liquid marbles.

2.2.3 Preparation of liquid marble hydrogels. First, the SA and GE of equal mass were dissolved in 20 mL water and stirred at 60 °C overnight to obtain sodium alginate-gelatin solution (SA-GE). After that, pyrethrin was added. Then, the above solution was homogenized at 10 000 rpm for 5 minutes to obtain a pyrethrin emulsion (Py-SA-GE) at concentrations ranging from 2.1% to 12.5% (w/v). As the internal solution, the

pyrethrin emulsion was dropped onto the modified cellulose powder to prepare the liquid marbles. Subsequently, liquid marbles loaded with pyrethrin were placed on the surface of the 5% $CaCl_2$ solution to obtain liquid marble hydrogels loaded with pyrethrin (Py-LM-Gels). Finally, the liquid marble hydrogels were transferred into a freeze dryer for ice sublimation for 12 h. The blank liquid marble hydrogels (LM-Gels) were prepared without adding pyrethrin. For comparison with liquid marble hydrogels, conventional calcium alginate hydrogels were also prepared by dropping Py-SA-GE and SA-GE into a 5% $CaCl_2$ solution.

2.3 Pesticide loading capacity

To assess the percentage loading (PL%) and percentage entrapment efficiency (EE%) of the Py-LM-Gels, the content of pyrethrin in the Py-LM-Gels was detected using a T6 UV/VIS spectrophotometer. The Py-LM-Gels were ground in a mortar and then immersed in 5 mL of methanol. The suspension was sonicated for 1 h and centrifuged at 8000 rpm for 5 min. After that, the supernatant absorbance of UV analysis was recorded at 230 nm.[36] The whole process was conducted under light-proof conditions. The drug carrier without pyrethrin has no influence on absorbance at 230 nm (Fig. S1†). The standard curve, which is used to calculate the amount of pyrethrin, is shown in Fig. S2.† The calculated formulas of PL% and EE% of the Py-LM-Gels are as follows:

$$\mathrm{PL}(\%)=\frac{\text{Total mass of pyrethrins in Py-LM-Gel}}{\text{Total mass of Py-LM-Gel}}\times 100\%, \quad (1)$$

$$\mathrm{EE}(\%)=\frac{\text{Total mass of pyrethrins in Py-LM-Gel}}{\text{Total mass of pyrethrins}}\times 100\%. \quad (2)$$

2.4 Release studies

2.4.1 Analysis of release mechanism. To study the release properties of Py-LM-Gels, 5 Py-LM-Gels were placed in a dialysis bag. Both ends of each dialysis bag were wired tightly, and the bag was placed into a beaker containing 30 mL of methanol–water (1 : 1, v : v) at a fixed temperature. All samples were shaken mildly in the dark. 100 μL of the released medium was removed at different time intervals (1, 2, 4, 6, 8, 10, 12, 24, 48, 72, 96, 120 and 144 h), and the absorbance using UV–VIS spectrometer was detected at 230 nm. An equal volume of fresh medium was added after sampling. The pyrethrin in the dissolved medium was calculated using the pyrethrin standard curve (Fig. S3†). For comparison, the release properties of the equivalent pyrethrin technology were investigated in the same way. The release rate of pyrethrin was calculated by applying eqn (3) as follows:

$$\text{Cumulative release}(\%)=\frac{C_nV+\sum_{i=0}^{n-1}C_{n-1}\times V_i}{W_0\times \mathrm{PL}\%}\times 100\%, \quad (3)$$

where C_n (mg mL^{-1}) and C_{n-1} (mg mL^{-1}) represent the concentrations of pyrethrin at n and $n-1$ times, respectively. V (mL) represents the volume of the release medium. V_i (mL) represents the volume taken out at $n-1$ time. W_0 (g) represents the weight of the liquid marble gels before swelling. The release kinetics of pyrethrin from the liquid marble hydrogels were investigated using zero order (eqn (4)), first order (eqn (5)), and Higuchi (eqn (6)) and Rigter–Peppas (eqn (7)) models:

$$\frac{M_t}{M_\infty}=Kt, \quad (4)$$

$$\frac{M_t}{M_\infty}=1-e^{-Kt}, \quad (5)$$

$$\frac{M_t}{M_\infty}=Kt^{1/2} \quad (6)$$

$$\frac{M_t}{M_\infty}=Kt^{n} \quad (7)$$

where M_t (mg) represents the cumulative release amount at time t. M_∞ (mg) represents the total amount of Py-LM-Gels. K is the characteristic constant and n represents the diffusion index.

2.4.2 Effects of temperature on release behavior. Considering that the mosquito eggs quickly hatched into larvae when the temperature was between 22 °C and 28 °C,[17] 20 °C was set as the lowest temperature for the release study. In addition, the degradation rate of pyrethrin is accelerated when the temperature exceeds 32 °C. Given the potential degradation of the released pyrethrin, 30 °C was set as the highest temperature for the release study. The experimental procedure and other conditions are identical to Subsubsection 2.4.1.

2.4.3 The effects of drug concentration on release behavior. Our research showed that the concentration of pyrethrin can affect the stability of pyrethrin emulsion and the preparation of liquid marble hydrogels (Fig. S4 and Table S2†). To verify whether drug release behavior was affected by the concentration of pyrethrin, pyrethrin emulsions of different concentrations (2.5%, 5.0% and 7.5%) were used to prepare liquid marble hydrogels for drug release experiments. The experimental procedure is identical to Subsubsection 2.4.1.

2.5 Stability

2.5.1 Stability in floating. The Py-LM-Gels were placed on the water surface. Then, the number of floating samples at fixed time intervals was counted. For comparison, the Py-Gels were also investigated. The flotation degree was calculated by eqn (8) as follows:

$$\text{Flotation degree}\ (\%)=\frac{\text{Number of floating samples over time}}{\text{Number of initial samples}}\times 100\%. \quad (8)$$

2.5.2 Storage stability. The prepared Py-LM-Gels were stored in a refrigerator (4 °C) for 6 months. Simultaneously, the morphology of Py-LM-Gels and the content changes in pyrethrin were investigated.

2.6 Application

2.6.1 Larvicidal activity test. Mortality was assumed for those wigglers that failed to move and turned red (Fig. S5 and ESI Video 1†). Py-LM-Gels (10, 30, and 60) were placed in 300 mL of lake water containing 10 *Aedes albopictus* larvae. The larvicidal performance at 24 h and 48 h was monitored without changing the water but with fresh larvae. LM-Gels were used as a control. The experiments were performed in three replicates.

2.6.2 Effect of water volume. In this study, the potential of Py-LM-Gels was explored, as a green slow-release formulation for mosquito larvae control with less dose. To confirm the effect of Py-LM-Gels in different volumes of water, the mortality of the wigglers in two beakers with different volumes of water was investigated. 10 Py-LM-Gels were placed in the beaker containing lake water (50 and 300 mL) and 10 *Aedes albopictus* larvae. The larvicidal performance of these larvae was monitored for a period without changing the water and larvae. LM-Gels were used as a control. The experiments were performed in three replicates.

2.6.3 Duration of drug action. 10 Py-LM-Gels were placed in 300 mL of lake water containing 10 *Aedes albopictus* larvae. The larvicidal performance was monitored without changing the water but with fresh larvae. For comparison, the same number of LM-Gels and the equivalent pyrethrin technology was investigated similarly. The experiments were performed in three replicates.

3. Results and discussion

3.1 Characterization

3.1.1 Characterization of cellulose. The synthesis process of the modified cellulose is illustrated in Fig. 1. The synthetic process involves the silanization of cellulose. The above-modified cellulose was assessed for its water contact angles. The levels of all factors are shown in Table S1.†

As shown in Fig. 2(A), the WCA of modified cellulose is highest when the volume of NaOH is 9 mL. Therefore, 9 mL NaOH was selected as the optimal condition. Similarly, 90 min and 80% ethanol concentrations were selected as the optimum conditions for the modification of cellulose (Fig. 2(B) and (C)).

As shown in Fig. 2(D), the WCAs of cellulose with different ratios of cellulose-VTES were not significantly different.

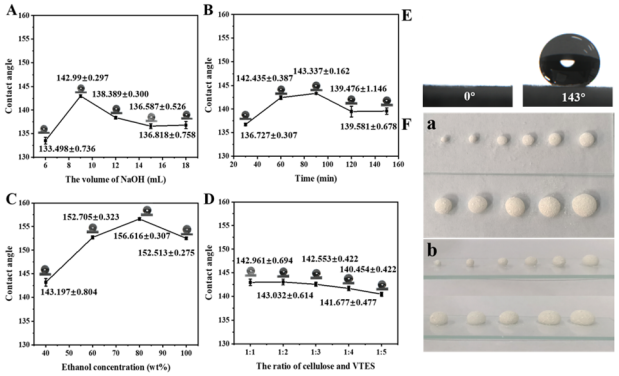

Fig. 2 (A) Effect of the volume of NaOH on the WCAs of modified cellulose; (B) effect of the time on the WCAs of modified cellulose; (C) effect of ethanol concentration on the WCAs of modified cellulose; (D) effect of the ratio of cellulose and VTES on the WCAs of modified cellulose; (E) water contact angle on cellulose powders before and after modification; (F) overhead view (a) and primary view (b) of liquid marble prepared using modified cellulose.

Considering environmental protection, cellulose-VTES (1 : 1, w : w) was selected as the optimum condition. The number of silane groups in silanized cellulose was 8.54 μmol g^{-1} determined by applying an Inductively Coupled Plasma Mass Spectrometer (ICP-MS).

The contact angle is the basic measurement used to estimate the wettability of a surface. The WCAs correlate with surface energy, which determines whether the powder can be used to prepare liquid marbles. Fig. 2(E) shows the WCAs of the cellulose before and after modification (0° → 143°). The surface energy of silanized cellulose is 56.93 mJ m^{-2}, which is calculated from the contact angle of silanized cellulose powder with formamide (31.831° ± 0.550) (Fig. S6†) and WCA. Fig. S7† illustrates the dispersion of silanized cellulose in different solvents, where it can be observed that the modified cellulose floats on the surface of the water owing to its excellent hydrophobicity while settling to the bottom in less polar solvents. Fig. 2(F) presents the images of liquid marbles with different volumes prepared by modified cellulose, demonstrating that modified cellulose is sufficiently hydrophobic to carry out subsequent experiments.

The FT-IR spectrum of the cellulose before and after modification is shown in Fig. 3(a) and (b). The bands at 3063 and

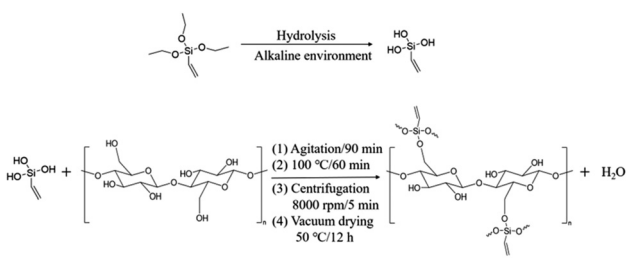

Fig. 1 Preparation process of modified cellulose.

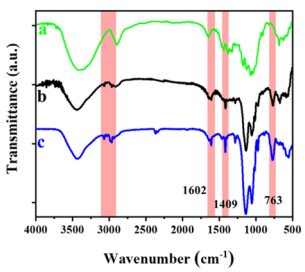

Fig. 3 FT-IR spectra of cellulose (a), modified cellulose (b) and VTES (c).

2960 cm^{-1} in Fig. 3(b) originate from the C–H stretching vibration and unsaturated alkene bonding. The band at 1602 cm^{-1} can be attributed to the C=C stretching vibration. The band at 1409 cm^{-1} is attributed to the in-plane deformation vibration of the vinyl. In addition, the Si–O–C band at 763 cm^{-1} confirms the successful preparation of modified cellulose.[37] The above results illustrated that the cellulose was modified by VTES. VTES can be hydrolyzed to yield vinylsilanetriol in an alkaline environment,[38] following which the cellulose is silanized by vinylsilanetriol, as shown in Fig. 1. Silanized cellulose, meanwhile, has high hydrophobicity,[39] interfacial bonding, and environmental durability[40,41] owing to the introduction of silyl groups.

3.1.2 Characterization of liquid marble. There are three types of liquid marbles prepared with water: SA-GE and pyrethrin emulsion. As shown in Fig. 4(A) and (B), the stability of these liquid marbles in air and water was obviously different. Owing to the introduction of pyrethrin, the surface energy of the internal solution changed, leading to a rupture of the liquid marbles. To overcome the instability of liquid marbles with pyrethrin, they were further prepared as liquid marble hydrogels by cross-linking with Ca^{2+}. The comparison of stability before and after cross-linking is shown in ESI video 2.†

3.1.3 Characterization of liquid marble hydrogel. There are some small gaps on the shell of liquid marbles. Therefore, the external Ca^{2+} in the $CaCl_2$ solution can enter liquid marble by water exchange and cross-linking with Sodium Alginate (SA). To visualize the cross-linking process, methylene blue was added to the 5% $CaCl_2$ solution, and the liquid marbles were removed after 60 min and frozen (Fig. 4(D)). As depicted in Fig. 4(D, insert c), from the bottom up, the color of the liquid marble changed from dark to light. The color change indicates that Ca^{2+} cross-linked with SA from the bottom up. Because of the existence of pyrethrin, it is inevitable that the shell of the liquid marble is gradually saturated. However, the stability of the liquid marbles is greatly increased owing to the cross-linking of Ca^{2+} and SA; thus, they remain stable on the water surface for a long time (Fig. 4(C)). Furthermore, the liquid marble hydrogels can rebound and maintain their initial shape in a drop impact test at a height of 15 cm (ESI Video 3†), which confirms that liquid marble hydrogel has a robust performance and makes these liquid marble hydrogels a hopeful prospect for practical applications. Moreover, as shown in Table 1, PY-SA-GE has green advancements, such as natural and green sources of raw materials, mild and non-polluting preparation processes, biodegradable and low cost compared with other reported drug release carriers.

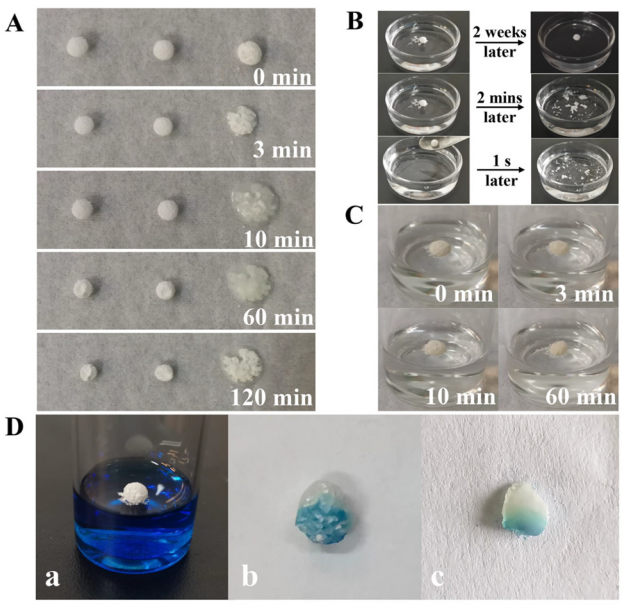

Fig. 4 (A) Digital images of liquid marble prepared using water, SA-GE and Py-SA-GE (from left to right) in the air; (B) digital images of liquid marble prepared using water, SA-GE and Py-SA-GE (from top to bottom) on water; (C) liquid marble with Py-SA-GE cross-linking on the $CaCl_2$ solution; (D) cross-linking visualization: the liquid marble is cross-linking on the $CaCl_2$ solution containing methylene blue (a), uncut Py-LM-Gel (b) and sliced Py-LM-Gel (c).

As illustrated in Fig. 5(A), the appearance of the liquid marble hydrogels and conventional calcium alginate hydrogels was different. The cellulose shell makes both types of liquid marbles (loaded and unloaded pyrethrin) appear white. The micromorphology of LM-Gels, Py-LM-Gels, conventional calcium alginate hydrogels (Gels) and conventional calcium alginate hydrogels loaded pyrethrin (Py-Gels) were observed by SEM. The surfaces of the LM-Gels and Py-LM-Gels were covered by cellulose microspheres (Fig. 5(A)), which are hydrophobic and give them the ability to float on the water surface. The surfaces of the Gels have many folds, which may be caused by volume shrinkage after freeze-drying.[24] Meanwhile, the surfaces of the Py-Gels were uneven, but no distinct folds were formed, which means that the addition of pyrethrin influenced the morphology of the hydrogels.

The FT-IR spectrum of pyrethrin technology showed a distinctive characteristic peak at 1717 cm^{-1} (Fig. 5(B, insert a)) attributed to the stretching vibration of C=O. Compared to LM-Gels (Fig. 5(B, insert c)), FT-IR analysis confirmed the presence of C=O in Py-LM-Gels (Fig. 5(B, insert b)) at 1717 cm^{-1}, which indicated that pyrethrin was successfully loaded into the material.

The thermal decomposition processes of pyrethrin technology, LM-Gels, and Py-LM-Gels are depicted in Fig. 5(C). The weight loss of LM-Gels and Py-LM-Gels was below 100 °C because of the water loss. The first mass loss of pyrethrin technology occurred in the range of 120–200 °C. Mass loss of LM-Gels and Py-LM-Gels mainly occurred in the range of 200–500 °C. The thermal decomposition of SA was reported to occur in the range of 200–280 °C, primarily caused by the breakage of its uronic and glucuronic acid segments.[24] In addition, the cellulose on the surface of LM-Gels and Py-LM-Gels is pyrolyzed in the range of 280–500 °C, undergoing dehydration, decarbonization and glycosidic bond breaking reactions. These processes generate small molecules of gas and large condensed volatile components, resulting in a rapid increase in mass loss. Compared to pyrethrin technology, Py-

Table 1 Comparison of PY-SA-GE developed in this study with other drug release carriers

Drug release carriers	Reaction condition	Sources of raw materials	Degradability	Ref.
MCM-48	Room temperature, 24 h; 550 °C, 5 h; 110 °C, N2 reflux, 24 h.	CATB, Pluronic F127, TEOS, MPTMS, APTS, TMCS	Not degradable	45
LC@UiO-66 nanoparticle	120 °C, 24 h; room temperature, 24 h.	$ZrCl_4$, H_2BDC	Not degradable	46
Ace@MSN-SS-C10	80 °C, 24 h; 600 °C, 5 h; room temperature, 24 h; 80 °C, 24 h.	CATB, Milli-Q, TEOS, MPTMS, GSH	Not degradable	47
PEG/MPTMS composite nanocarrier	Room temperature, 24 h; 85 °C, 24 h; 140 °C, 24 h.	h-BN, PEG, MPTMS	Not degradable	48
CAP@MIL-101(Fe)@silica	120 °C, 12 h; room temperature, 24 h.	$FeCl_3$, BDC, $Na_2SiO_3{\cdot}9H_2O$	Not degradable	49
Py-SA-GE	Room temperature, 1.5 h; 100 °C, 1 h; 60 °C, 12 h.	cellulose, VTES, sodium alginate	Degradable	This work

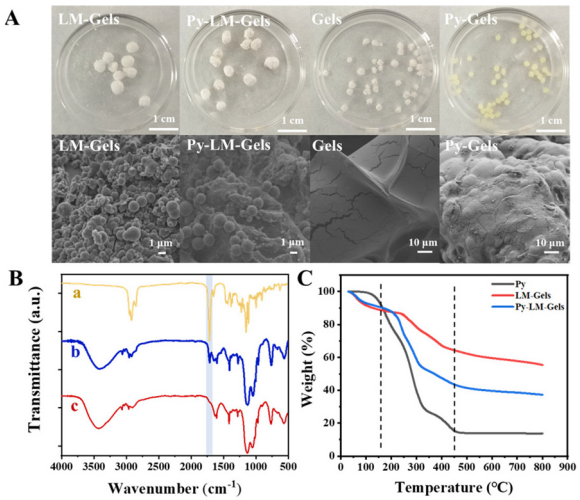

Fig. 5 (A) Digital images and SEM images of LM-Gels, Py-LM-Gels, Gels and Py-Gels; (B) FT-IR spectra of pyrethrin technology (a), Py-LM-Gels (b) and LM-Gels (c); (C) TGA curve of pyrethrin technology, LM-Gels and Py-LM-Gels.

LM-Gels shift backwards in the range of 200–500 °C, indicating that the thermal decomposition temperature tends to be higher. In other words, Py-LM-Gels have a higher thermal stability than pyrethrin, which can mitigate the degradation of pyrethrin. Compared to LM-Gels, the lower inflection temperature of Py-LM-Gels at 200–300 °C suggested that the presence of pyrethrin may have caused minor changes to the internal structure of the liquid marble gels. From 500 to 800 °C, the mass losses of pyrethrin technology, LM-Gels, and Py-LM-Gels tend to be stable.

3.2 Optimization of preparation conditions

3.2.1 Optimization of pyrethrin emulsion. The stability of the emulsion may affect the uniformity of drug distribution in liquid marble hydrogels. An interaction exists between the $-NH_2$ group of GE and the COO^- group of SA,[24] which is beneficial to the stability of the pyrethrin emulsion. Therefore, to prepare pyrethrin emulsion, GE and SA solutions were selected as the water phase. To finalize the range of conditions in the next step of the reaction, the influence of the concentrations of SA-GE and pyrethrin on emulsion stability was discussed. As illustrated in Fig. S4(a),† the emulsions were layered within 24 h when the concentration of the SA-GE solution was lower than 2.0%. In practice, when the concentration of SA-GE was greater than 2.5%, the liquid became too viscous to control the volume. Therefore, the concentration of the SA-GE solution can be between 2.0% and 2.5%. As shown in Fig. S4(b),† the pyrethrin emulsions were stable at all studied pyrethrin concentrations (2.1–12.5%, w/v), which proved that the experiment could be conducted in the concentration range.

3.2.2 Optimization of liquid marble hydrogel. The effects of the concentration of SA-GE, pyrethrin and $CaCl_2$ solution on the formation of liquid marble hydrogels and drug loading properties were investigated. As illustrated in Fig. 6(A) and Table 2, the PL% increased from 6.8% in the case of 1.5% SA-GE to a maximal value of 11.7% in the case of 2.0% SA-GE; simultaneously, the EE% also increased. This phenomenon could be attributed to the increasing viscosity with increasing SA-GE concentration, which maintained pyrethrin emulsion stability to prevent drug loss. However, as the SA-GE concentration was above 2.0%, the PL decreased significantly.

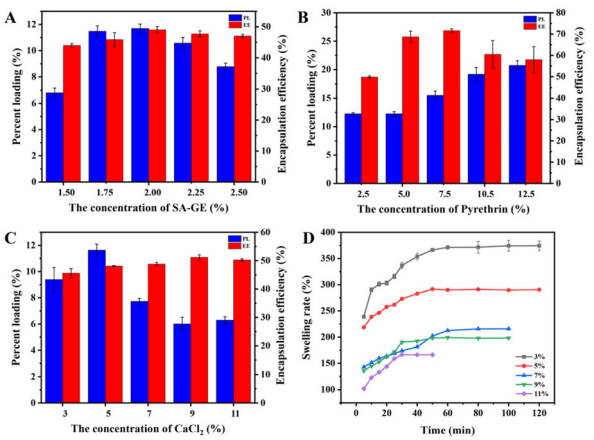

Fig. 6 (A) Effect of SA-GE concentration on PL% and EE%; (B) effect of pyrethrin concentration on PL% and EE%; (C) effect of $CaCl_2$ concentration on PL% and EE%; (D) swelling study of Py-LM-Gels.

Table 2 PL% and EE% of the prepared Py-LM-Gels

Concentration of SA-GE (%)	Concentration of $CaCl_2$ (%)	Concentration of pyrethrin (%)	PL (%)	EE (%)
1.50	5	2.5	6.8 ± 0.4	44.0 ± 0.5
1.75	5	2.5	11.5 ± 0.4	45.9 ± 2.2
2.00	5	2.5	11.7 ± 0.3	49.1 ± 1.0
2.25	5	2.5	10.6 ± 0.4	47.7 ± 1.0
2.50	5	2.5	8.8 ± 0.3	47.0 ± 0.5
2.00	3	2.5	9.4 ± 0.9	45.6 ± 1.6
2.00	5	2.5	11.6 ± 0.6	48.1 ± 0.2
2.00	7	2.5	7.7 ± 0.2	48.8 ± 0.5
2.00	9	2.5	6.0 ± 0.5	51.2 ± 0.9
2.00	11	2.5	6.3 ± 0.3	50.3 ± 0.4
2.00	5	2.5	12.3 ± 0.2	49.8 ± 0.5
2.00	5	5.0	12.6 ± 0.4	68.6 ± 2.6
2.00	5	7.5	15.5 ± 0.8	71.6 ± 0.8
2.00	5	10.0	19.2 ± 1.2	60.5 ± 6.5
2.00	5	12.5	20.7 ± 0.8	58.0 ± 6.1

Therefore, 2.0% was selected as the SA-GE concentration for the preparation of liquid marble hydrogels.

The PL% increases with the increase in pyrethrin concentration (Fig. 6(B)). However, the EE% increased considerably when the concentration of pyrethrin was higher than 7.5%. Therefore, these concentrations (2.5%, 5% and 7.5%) were selected to prepare the liquid marble hydrogels for subsequent release experiments, as the optimized condition.

As illustrated in Fig. 6(C) and Table 2, when the concentration of the $CaCl_2$ solution was lower than 5%, the crosslinking time was too long, leading to pesticide loss. When the $CaCl_2$ concentration was more than 5%, the PL% began to decrease. This is because a high concentration of $CaCl_2$ solution leads to excessive cross-linking in the unit time, resulting in a higher density. To confirm this hypothesis, the swelling aptitude of these samples made under the above 5 conditions was evaluated by gravimetry, as shown in Fig. 6(D). The swelling behavior of Py-LM-Gels is observed to be related to the concentration of the $CaCl_2$ solution: the swelling equilibrium rates decreased as the concentration of the $CaCl_2$ solution increased. This is consistent with the reported results.[42] Furthermore, too many crosslinking agents may cause drug release to be inhibited. Therefore, 5% was selected as the optimum condition for the preparation of liquid marble hydrogels.

3.3 Release studies

3.3.1 Analysis of the release mechanism. The release behaviors of pyrethrin technology and Py-LM-Gels are shown in Fig. 7(A). Obviously, the pyrethrin technology showed a rapid release, with a burst effect of about 90% in a very short period and completely released within 24 h. In contrast, Py-LM-Gels displayed outstanding slow-release properties. Furthermore, the pyrethrin technology was still released from the Py-LM-Gels even after 144 h. During the initial 24 h, a cumulative release of 45.2% was obtained, and the release process of the Py-LM-Gels was relatively fast. Then, the release speed tends to slow down. As a slow-release material, the benefit of an appropriate rapid release at an early stage is that the increased initial drug release amount can provide better control efficiency.[43] To further investigate the release mechanism of Py-LM-Gels, four release models were used (Fig. 7(B) and Table 3).

Among them, the first-order model was the best-fitted theoretical model (R^2 = 0.9836). In addition, the release data correlated well with those of Ritger–Peppas and Higuchi. It is clear from the Ritger–Peppas model equations that the mechanism of drug release involves case II transport ($n \geq 0.85$), non-Fickian transport ($0.43 < n < 0.85$) and Fickian diffusion ($n \leq 0.43$).[44] The calculated value of n is 0.65, suggesting that the release is caused by non-Fickian diffusion, including swelling of hydrogels by water absorption and slackening of the SA chains. Comparable results of the kinetic parameters were found at different temperatures and pyrethrin concentrations (Table S3†).

3.3.2 Effects of temperature on release behavior. When the temperature increased, the release rate of pyrethrin from the liquid marble hydrogels was slightly enhanced (Fig. 7(C)). This may be attributed to the fact that the increased temperature promotes swelling of the liquid marble hydrogels and accelerates molecular movement, which is consistent with the release mechanism of the Py-LM-Gels. The release behavior of pyrethrin technology was similar at two different temperatures (Table S3†), demonstrating that temperature insignificantly affected the Py-LM-Gels release behaviors. In other words, Py-LM-Gels can provide a stable release of pyrethrin in a temperature range that is suitable for mosquito larvae.

3.3.3 Effects of drug concentration on release behavior. As depicted in Fig. 7(D), the Py-LM-Gels prepared with different

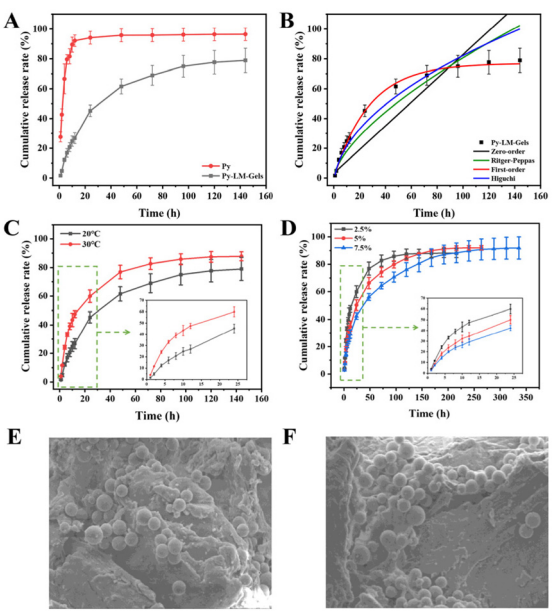

Fig. 7 (A) Cumulative release rate of Py and Py-LM-Gels; (B) four release model curves of Py-LM-Gels; (C) cumulative release rate of Py-LM-Gels at 20 and 30 °C; (D) cumulative release rate of Py-LM-Gels prepared using pyrethrin emulsion with different concentrations; SEM images of Py-LM-Gels before (E) and after (F) release.

Table 3 The kinetic parameters and equation of pyrethrin released from Py-LM-Gels

Model	Equation	R^2
Zero-order	$Y = 3.1998 + 0.7965t$	0.7631
First-order	$Y = 76.9936(1 - e^{-0.0366t})$	0.9883
Higuchi	$Y = 8.9104t^{1/2}$	0.9718
Ritger–Peppas	$Y = 3.9925t^{0.6527}$	0.9091

concentrations of pyrethrin emulsions take different times to reach equilibrium for drug release. This result indicates that the effective time of the Py-LM-Gels may be influenced by the concentration of pyrethrin emulsions. The higher the pyrethrin emulsion concentration, the higher the pyrethrin concentration in the Py-LM-Gels. The increase in pyrethrin in the carrier lengthens the release time. The cumulative release of the Py-LM-Gels prepared by the 7.5% pyrethrin emulsion still increased slowly after 336 h. In addition, there was no significant variation in the appearance of Py-LM-Gels before and after release (Fig. 7(E) and (F)), which showed the good stability of the drug carrier.

3.4 Stability

As shown in Fig. 8(A) and (B), owing to the hydrophobic cellulose on the surface, the Py-LM-Gels can float stably on water for more than 24 h. The floating rate did not decrease until after 48 h. In contrast, the Py-Gels without hydrophobic cellulose immediately sunk to the bottom. Additionally, Py-LM-Gels can be easily removed from water after use.

In practical applications, the stability of storage is extremely crucial. Hence, the appearance and pyrethrin content of Py-LM-Gels over a period of 6 months were investigated. It is evident in Fig. 8(C) that the content of all samples remained stable without a significant decrease in concentration or significant changes in appearance.

3.5 Application

3.5.1 Larvicidal activity test. As shown in Table 4, with an increase in the number of Py-LM-Gels, the mortalities of *Aedes albopictus* larvae increased during the same period. The results indicate that the larvicidal activity of Py-LM-Gels can be controlled by the number of Py-LM-Gels. There is no death of the mosquito larvae in the LM-Gels group during the whole experimental period.

3.5.2 Effect of water volume. The larvicidal activity of Py-LM-Gels to *Aedes albopictus* larvae in beakers with different volumes of water was evaluated. As depicted in Table 5, the larval mortalities of the two beakers reached 100% within 24 h and 48 h. The water volume of beaker-2 is 6 times larger than beaker-1, while the larvicidal activity of water system-2 can still reach 100%. This is because the Py-LM-Gels are floating on the water surface, leading to the highest concentration of pyrethrin on the surface of the water, where mosquito larvae happen to live (ESI Video 4†). These results suggested that Py-LM-Gels based on the habit of larvae can improve the utilization of pyrethrin effectively, thereby reducing the cost of applying pesticide.

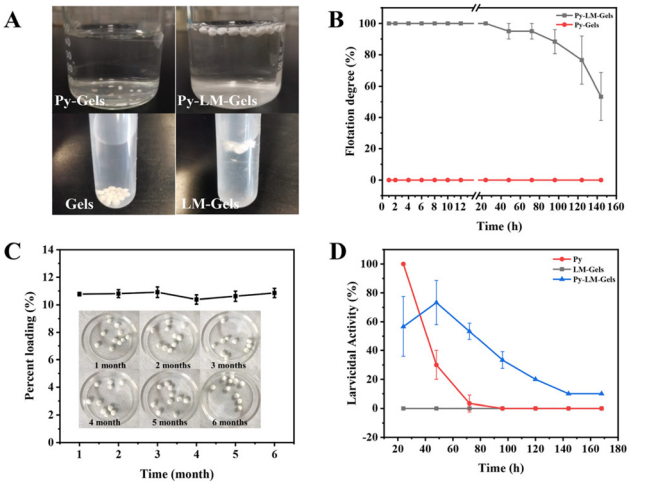

Fig. 8 (A) Digital images of Py-Gels, Gels, Py-LM-Gels and LM-Gels in the water; (B) the flotation degree of LM-Gels and Py-LM-Gels; (C) long-term storage stability of Py-LM-Gels; (D) duration of drug action of Py, LM-Gels and Py-LM-Gels.

Table 4 Larvicidal activity of Py-LM-Gels

		Larvicidal activity (%, Mean ± S.E, $N = 3$)		
Sample	Time (h)	10[a]	30[a]	60[a]
LM-Gels	24	0	0	0
Py-LM-Gels		40.0 ± 10.0	56.6 ± 20.8	100
LM-Gels	48	0	0	0
Py-LM-Gels		70	73.3 ± 15.3	100

[a] Number of Py-LM-Gels used.

Table 5 Larvicidal activity in different sizes of water systems

	Larvicidal activity (%, Mean ± S.E, $N = 3$)		
Sample	24[a]	48[a]	72[a]
Control	0	0	0
Beaker-1	66.6 ± 20.8	100	—
Beaker -2	43.3 ± 15.2	70	100

[a] Time of Py-LM-Gels release. Beaker-1: contained 50 mL of lake water. Beaker-2: contained 300 mL of lake water.

3.5.3 Duration of drug action. It can be observed from Fig. 8(D) that, initially, the virulence of pyrethrin technology to larvae was considerably higher than that of Py-LM-Gels. However, the larval mortalities of pyrethrin technology decreased rapidly and reached 3.3% after 72 h. In contrast, with the release time extending from 24 to 48 h, the number of dead larvae in the Py-LM-Gel group continued to increase. The larvicidal activity of Py-LM-Gels started to decrease slowly only after 48 h. Furthermore, the Py-LM-Gels maintained larvicidal

performance even after 168 h. The above results showed that the Py-LM-Gels were beneficial in extending the drug efficacy period and decreasing doses with their slow-release properties.

4. Conclusions

In this study, the habits of mosquito larvae and the characteristics of liquid marbles were exploited to design a green slow-release carrier by cross-linking Ca^{2+} and pyrethrin emulsion on the surface of the $CaCl_2$ solution. The liquid marble-based hydrogels showed well-intended features, such as good floatation, long sustained-release time, stable release of pyrethrin in the needed range of temperature and good storage stability. In addition, hydrogel carrier efficient mosquito larvae killing was witnessed with the same dosage of pyrethrin in beakers containing different volumes of water because the materials can release pyrethrin on the water surface. Subsequent investigations could concentrate on improving the reuse efficiency of liquid marble hydrogel drug carriers and utilizing biomass cellulose as a source of material for slow-release drug carriers to improve the sustainability of the introduction strategy. In summary, as a green slow-release drug carrier, this carrier can effectively kill wigglers and provide a new clue for expanding the application of liquid marbles.

Conflicts of interest

There are no conflicts to declare.

Acknowledgements

This work was financially supported by National Natural Science Foundation of China (81973451, 22208036), Fundamental and Frontier Research Fund of Chongqing (CSTB2023NSCQ-MSX0490, CSTC2019JSYJ-YZYSBAX0020, CSTC2018JCYJAX0661), the Science and Technology Research Program of Chongqing Municipal Education Commission (KJZD-K201800103), Fundamental Research Funds for the Central Universities (2019CDYGYB027, 2022CDJXY-003), Graduate Research and Innovation Foundation of Chongqing (CYS18033), Graduate Research and Innovation Project of Chongqing (CYB22041), Venture & Innovation Support Program for Chongqing Overseas Returnees (CX2019117).

References

1 F. Liu, Q. Wang, P. Xu, F. Andreazza, W. R. Valbon, E. Bandason, M. Chen, R. Yan, B. Feng, L. B. Smith, J. G. Scott, G. Takamatsu, M. Ihara, K. Matsuda, J. Klimavicz, J. Coats, E. E. Oliveira, Y. Du and K. Dong, *Nat. Commun.*, 2021, **12**, 2553.
2 K. Murugan, G. Benelli, S. Ayyappan, D. Dinesh, C. Panneerselvam, M. Nicoletti, J. S. Hwang, P. M. Kumar, J. Subramaniam and U. Suresh, *Parasitol. Res.*, 2015, **114**, 2243–2253.
3 C. L. Silva-Inacio, A. A. Pereira De Paiva, J. M. Galvao De Araujo and M. D. F. Freire De Melo Ximenes, *Rev. Soc. Bras. Med. Trop.*, 2020, **53**, e20200502.
4 Y. H. Zhou, Z. W. Zhang, Y. F. Fu, G. C. Zhang and S. Yuan, *Front. Behav. Neurosci.*, 2018, **12**, 00086.
5 G. Benelli, *Parasitol. Res.*, 2015, **114**, 3201–3212.
6 K. Murugan, D. Nataraj, P. Madhiyazhagan, V. Sujitha, B. Chandramohan, C. Panneerselva, D. Dinesh, R. Chandirasekar, K. Kovendan, U. Suresh, J. Subramaniam, M. Paulpandi, C. Vadivalagan, R. Rajaganesh, H. Wei, B. Syuhei, A. T. Aziz, M. S. Alsalhi, S. Devanesan, M. Nicoletti, A. Canale and G. Benelli, *Parasitol. Res.*, 2016, **115**, 1071–1083.
7 H. A. E.-K. Bosly, N. Salah, S. A. Salama, R. A. Pashameah and A. Saeed, *Acta Trop.*, 2023, **237**, 106735.
8 N. Parvin, T. K. Mandal, P. C. Nagajyothi, P. M. Reddy, N. R. Reddy and S. W. Joo, *J. Cluster Sci.*, 2021, **32**, 1761–1767.
9 E. V. Minello, F. Lai, M. T. Zonchello, M. Melis, M. Russo, P. Cabras and J. Agric, *Food Chem.*, 2005, **53**, 8302–8305.
10 J. Shin, S.-M. Seo, I.-K. Park and J. Hyun, *Carbohydr. Polym.*, 2021, **254**, 117381.
11 B. L. Atkinson, A. J. Blackman, H. Faber and J. Agric, *Food Chem.*, 2004, **52**, 280–287.
12 N. Jeran, M. Grdisa, F. Varga, Z. Satovic, Z. Liber, D. Dabic and M. Biosic, *Phytochem. Rev.*, 2021, **20**, 875–905.
13 M. Fernández-Pérez, F. Flores-Céspedes, I. Daza-Fernández, F. Vidal-Peña and M. Villafranca-Sánchez, *Ind. Eng. Chem. Res.*, 2014, **53**, 13557–13564.
14 M. Massaro, S. Pieraccini, S. Guernelli, M. L. Dindo, S. Francati, L. F. Liotta, G. C. Colletti, S. Masiero and S. Riela, *Appl. Clay Sci.*, 2022, **230**, 106719.
15 A. Kalaitzaki, N. E. Papanikolaou, F. Karamaouna, V. Dourtoglou, A. Xenakis and V. Papadimitriou, *Langmuir*, 2015, **31**, 5722–5730.
16 N. E. Papanikolaou, A. Kalaitzaki, F. Karamaouna, A. Michaelakis, V. Papadimitriou, V. Dourtoglou and D. P. Papachristos, *Environ. Sci. Pollut. Res.*, 2018, **25**, 10243–10249.
17 Y. Zhang, W. Chen, M. Jing, S. Liu, J. Feng, H. Wu, Y. Zhou, X. Zhang and Z. Ma, *Chem. Eng. J.*, 2019, **361**, 1381–1391.
18 J. Xu, Y. He, Y. Li and Q. Ye, *Mater. Lett.*, 2020, **260**, 126968.
19 Q.-Q. Wang, Y. Liu, C.-J. Zhang, C. Zhang and P. Zhu, *Mater. Sci. Eng., C*, 2019, **99**, 1469–1476.
20 Y. Xiang, X. Lu, J. Yue, Y. Zhang, X. Sun, G. Zhang, D. Cai and Z. Wu, *Sci. Total Environ.*, 2020, **722**, 137811.
21 Z. Rahiminezhad, H. H. Gahruie, S. Esteghlal, G. R. Mesbahi, M.-T. Golmakani and S. M. H. Hosseini, *LWT–Food Sci. Technol.*, 2020, **127**, 109392.
22 A. Tanwar, P. Date and D. Ottoor, *J. Colloid Interface Sci.*, 2021, **42**, 100413.
23 J. Douliez, A. Perro, J. Chapel, B. Goudeau and L. Beven, *Small*, 2018, **14**, 1803042.

24 J. Xing, W. Dang, J. Li and J. Huang, *Colloids Surf., B*, 2021, **204**, 111776.
25 S. Fujii, S.-I. Yusa and Y. Nakamura, *Adv. Funct. Mater.*, 2016, **26**, 7206–7223.
26 P. Aussillous and D. Quere, *Nature*, 2001, **411**, 924–927.
27 M. Uda, S. Higashimoto, T. Hirai, Y. Nakamura and S. Fujii, *Polymer*, 2021, **212**, 123295.
28 X. Lin, W. Ma, H. Wu, S. Cao, L. Huang, L. Chen and A. Takahara, *Chem. Commun.*, 2016, **52**, 1895–1898.
29 Z. Zhao, S. Qin, D. Wang, Y. Pu, J.-X. Wang, J. Saczek, A. Harvey, C. Ling, S. Wang and J.-F. Chen, *Chem. Eng. J.*, 2020, **391**, 123478.
30 S. Yukioka, J. Fujiwara, M. Okada, S. Fujii, Y. Nakamura and S.-I. Yusa, *Langmuir*, 2020, **36**, 6971–6976.
31 X. Luo, X. Zhang and Y. Feng, *Acta Phys. Sin.-Ch. Ed.*, 2020, **36**, 1–20.
32 T. Boleslavská, O. Rychecký, M. Krov, P. Žvátora, O. Dammer, J. Beránek, P. Kozlík, T. Křížek, J. Hořínková, P. Ryšánek, J. Roušarová, N. K. Canová, M. Šíma, O. Slanař and F. Štěpánek, *AAPS J.*, 2020, **22**, 1–12.
33 M. Arshadi, M. Azizi, H. Souzandeh, C. Tan, S. M. Davachi and A. Abbaspourrad, *J. Mater. Chem. A*, 2019, **7**, 26456–26468.
34 A. J. Leite, N. M. Oliveira, W. Song and J. F. Mano, *Sci. Rep.*, 2018, **8**, 15215.
35 Y. Kim, S. Oh, H. Lee, D. Lee, M. Kim, H. S. Baek, W. S. Park, E. Kim and J.-H. Jang, *Biomater. Sci.*, 2021, **9**, 1639–1651.
36 R. Yan, Q. Zhou, Z. Xu, Y. Wu, G. Zhu, M. Wang, Y. Guo, K. Dong and M. Chen, *Pest Manage. Sci.*, 2021, **77**, 3706–3712.
37 M. Beaumont, M. Bacher, M. Opietnik, W. G. Altmutter, A. Potthast and T. Rosenau, *Molecules*, 2018, **23**, 23061427.
38 Y. Wu, S. Jia, Y. Qing, S. Luo and M. Liu, *J. Mater. Chem. A*, 2016, **4**, 14111–14121.
39 H. Nakatani, K. Iwakura, K. Miyazaki, N. Okazaki and M. Terano, *J. Appl. Polym. Sci.*, 2011, **119**, 1732–1741.
40 E. E. Pérez, S. Domenek, N. Belgacem, C. Sillard and J. Bras, *Biomacromolecules*, 2014, **15**, 4551–4560.
41 B. P. Frank, D. P. Durkin, E. R. Caudill, L. Zhu, D. H. White, M. L. Curry, J. A. Pedersen and D. H. Fairbrother, *ACS Appl. Nano Mater.*, 2018, **1**, 7025–7038.
42 S. H. Ahn, M. Rath, C.-Y. Tsao, W. E. Bentley and S. R. Raghavan, *ACS Appl. Mater. Interfaces*, 2021, **13**, 18432–18442.
43 J. Luo, Y. Gao, Y. Liu, J. Du, D.-X. Zhang, H. Cao, T. Jing, B.-X. Li and F. Liu, *Nanoscale*, 2021, **13**, 15647–15658.
44 G.-B. Li, J. Wang and X.-P. Kong, *Carbohydr. Polym.*, 2020, **249**, 116865.
45 S. Xiao, A. Shoaib, J. Xu and D. Lin, *Sci. Total Environ.*, 2022, **831**, 154914.
46 W. Menga, Z. Tiana, P. Yao, X. Fang, T. Wub, J. Cheng and A. Zoua, *Colloids Surf., A*, 2020, **604**, 125266.
47 Y. Ding, Z. Xiao, F. Chen, L. Yue, C. Wang, N. Fan, H. Ji and Z. Wang, *Sci. Total Environ.*, 2023, **863**, 160900.
48 L. Hao, L. Gong, L. Chen, M. Guan, H. Zhou, S. Qiu, H. Wen, H. Chen, X. Zhou and M. Akbulut, *Chem. Eng. J.*, 2020, **396**, 125233.
49 Y. Gao, Y. Liang, Z. Zhou, J. Yang, Y. Tian, J. Niu, G. Tang, J. Tang, X. Chen, Y. Li and Y. Cao, *Chem. Eng. J.*, 2021, **422**, 130143.